

Ab initio tensile tests of Al bulk crystals and grain boundaries: universality of mechanical behaviour

Rebecca Janisch,* Naveed Ahmed, and Alexander Hartmaier
*Interdisciplinary Centre for Advanced Materials Simulation,
Ruhr-University Bochum, 44780 Bochum, Germany*

(Dated: January 13, 2021)

We have performed *ab initio* tensile tests of bulk Al along different tensile axes, as well as perpendicular to different grain boundaries to determine mechanical properties such as interface energy, work of separation and theoretical strength. We show that all the different investigated geometries exhibit energy-displacement curves that can be brought into coincidence in the spirit of the well known universal binding energy relationship curve. This simplifies significantly the calculation of *ab initio* tensile strengths for the whole parameter space of grain boundaries.

I. INTRODUCTION

The prediction of the mechanical properties of polycrystals requires knowledge about the mechanical properties of all interfaces, i.e. grain boundaries, in their microstructure. So far, most mesoscale models of microstructure-property relationships as used in continuum simulations of deformation and fracture make rather simple assumptions for the variation in grain boundary properties with the boundary geometry^{1,2}. With *ab initio* electronic structure calculations it is possible to determine the cohesive energy, elastic modulus, sliding barrier, and theoretical strength of interfaces accurately and quantitatively. The considerable computational effort, in comparison e.g. to atomistic simulations employing empirical potentials, is easily feasible with modern computers if the investigations are restricted to grain boundary structures based on coincidence-site lattices. The *ab initio* approach is desirable to avoid problems of transferability of empirical potentials, usually fitted to reproduce equilibrium properties, to non-equilibrium processes such as failure. It is indispensable whenever a phenomenon is controlled by the electronic structure. This is the case in systems with directional bonds, or when studying the influence of chemical composition, and alloying effects. Nevertheless, sampling the five parameter space given by the geometric degrees of freedom of the grain boundary (rotation axis and angle, and the grain boundary normal³) by *ab initio* calculations remains a challenge. Models exist that relate the energies of certain subsets of this space to the grain boundary geometry. Most well known is the dislocation model for small angle tilt grain boundaries based on the picture of Read and Shockley, which can be extended empirically to large-angle tilt grain boundaries⁴. If the energy of a grain boundary can be related to its geometric parameters via such models, the description of the energy hypersurface is significantly simplified. However, so far it seems that there is no such correlation which would be valid in the complete parameter space^{5,6}. The complexity of the problem is increased by the fact that for use in mesoscale models we are not only looking for a function that describes the grain boundary energy as function of misorientation,

but also for its first and second derivatives with respect to a displacement from the equilibrium volume, i.e. the maximum stress and the elastic modulus. Nevertheless, the situation is not hopeless, as the analytic function of this energy-displacement curve is the same for any grain boundary geometry, if obtained under the same loading conditions. The demonstration of this fact, a universal binding behaviour in the spirit of Rose's universal binding energy relationship (UBER)⁷, is subject matter of this paper.

In section II we describe our computational procedure, including an explanation of grain boundary nomenclature and details on different ways to perform "*ab initio*" tensile tests. In section III we review the UBER and its implications. In the results' section, sec. IV, we give details about the grain boundary structures after a full optimization of the microscopic degrees of freedom (IV A) and the corresponding energies (IV B). The results of the tensile tests are presented in section IV C. The universal elastic behaviour under tensile load of all systems investigated is demonstrated in section IV D, and the relationship between energies and strength is discussed in section IV E. We summarize our insights in section V.

II. TECHNICAL DETAILS

For a given orientation of the tensile axis, we constructed supercells for bulk, surface, and grain boundary calculations of the same size and shape. In other words, starting from a bulk supercell containing N atomic layers, half of the planes were replaced by vacuum to create a surface slab, or half of the planes were replaced by the same number, but with a misorientation, to create a grain boundary structure.

In detail, supercells for tensile tests were constructed for Al bulk, such that the z -axis is oriented along the [111], [112], [113], and [114] direction, i.e. defining (111), (112), (113) and (114) as the cleavage plane. In addition we constructed special grain boundaries containing these planes as grain boundary planes. These were the $\Sigma 3$ (111) [111] 60° twist grain boundary, the $\Sigma 3$ (1 $\bar{1}$ 2) [110] 109° symmetrical tilt grain boundary (STGB), the

Σ_{11} ($1\bar{1}3$) [110] 129° STGB, and the Σ_9 ($1\bar{1}4$) [110] 141° STGB. In this nomenclature the use of Σ indicates that for the chosen misorientation a periodic superstructure can be found, the so-called coincidence site lattice (CSL). Therefore these grain boundaries are also called special grain boundaries. The value of Σ is the volume of a unit of this CSL divided by the volume of the cubic Al unit cell, i.e. it is a measure for the periodicity of the grain boundary. The grain boundary plane is given in round brackets, the direction of the axis of misorientation in rectangular ones. All tilt grain boundaries considered here are symmetrical, which means that the grain boundary plane divides the misorientation angle in two equal parts. In other words, it represents a mirror plane. Note that the (111) [111] 60° twist grain boundary can also be expressed as (111) [110] 70.5° tilt grain boundary, but we prefer to refer to it as twist grain boundary to emphasize its close-packed atomic structure.

To calculate the total energy of the above mentioned supercells we performed density-functional-theory (DFT) calculations of total energy and electronic structure employing the ABINIT open source code⁸. The exchange correlation effects were treated in the local density approximation and electron-ion interactions were modeled via a Troullier-Martins type norm-conserving pseudopotential for Al. Convergence with respect to k -point density, plane wave energy cut-off, and system size was tested for the (111) surface energy. The surface energy is given by

$$\gamma_{\text{FS}} = \frac{2 \cdot E_{\text{tot}}^{\text{FS}} - E_{\text{tot}}^{\text{bulk}}}{4A} \quad (1)$$

where $E_{\text{tot}}^{\text{FS}}$ is the total energy of the surface slab and $E_{\text{tot}}^{\text{bulk}}$ the energy of the bulk supercell containing twice the number of atomic layers. A is the surface area. The plane wave cut-off was varied between 12 and 20 Ha in steps of 2 Ha. To test convergence with respect to cell size, we chose bulk (surface) supercells containing 18 (9), 24 (12), or 30 (15) (111) planes. The k -point meshes employed were of the Monkhorst-Pack type, using $2 \times 2 \times 1$, $4 \times 4 \times 1$, $8 \times 8 \times 2$, and $12 \times 12 \times 2$ k -points. With a plane wave cut-off of 16 Ha, the $8 \times 8 \times 2$ Monkhorst-Pack mesh, and a minimum surface slab thickness of nine atomic layers, the surface energy was converged within an accuracy of $1 \cdot 10^{-4}$ Ha/atom ($\approx 2.5 \cdot 10^{-3}$ eV/atom).

For orientations different from z parallel to [111] it was ensured that the distance between the interfaces was at least as large as in the [111] cells. The supercell shapes were made commensurate with that of the [111] cell, which also enables the use of a commensurate k -point mesh.

To obtain accurate interface energies all microscopic degrees of freedom were optimized and the positions of the atoms were relaxed until the remaining forces were smaller than $5 \cdot 10^{-5}$ Ha/a.u. ($\approx 3 \cdot 10^{-3}$ eV/Å). Afterwards, the excess interplanar spacing of the grain boundaries can be calculated as half the difference (due to the periodic boundary conditions) between the relaxed (D_0)

and initial (D_{hkl}) supercell length perpendicular to the interface,

$$d_0 = \frac{D_0 - D_{hkl}}{2} \quad (2)$$

The grain boundary energy is given by

$$\gamma_{\text{GB}} = \frac{E_{\text{tot}}^{\text{GB}} - E_{\text{tot}}^{\text{bulk}}}{2A} \quad (3)$$

where $E_{\text{tot}}^{\text{GB}}$ is the total energy of the grain boundary supercell and $E_{\text{tot}}^{\text{bulk}}$ the energy of the bulk supercell containing the same number of crystallographic layers in the corresponding orientation. A is the interface area. From the total energy of the surface slabs, also the work of separation of a grain boundary was calculated according to

$$W_{\text{sep}} = \frac{2 \cdot E_{\text{tot}}^{\text{FS}} - E_{\text{tot}}^{\text{GB}}}{2A} \quad (4)$$

Note that the work of separation for the perfect bulk corresponds to twice the surface energy as defined in eq. (1).

After a fit of the energy-displacement curves, the tensile strength can be calculated as the slope in the inflection point:

$$\sigma_{\text{th}} = \left. \frac{dE}{d\Delta} \right|_{E''(\Delta)=0} \quad (5)$$

where Δ is the displacement from the equilibrium interplanar distance. Initially, the tensile tests were performed in three different ways: (a) by a simple scaling of the supercell dimensions along the tensile axis, while leaving the internal coordinates fixed. Atomic relaxations then lead to a homogeneous strain distribution in bulk supercells, and a characteristic distribution of strain in any cell containing a defect (e.g. a grain boundary). (b) By performing rigid grain shifts (rgs). Here the spacing between two blocks of atoms is increased only at a defined cleavage plane (due to the use of periodic boundary conditions at two defined cleavage planes per supercell). Within the blocks, the interplanar distance corresponds to the equilibrium bulk value. This way we can model ideally brittle cleavage under loading mode I. (c) By doing the latter and relaxing the atomic positions at each shift, while keeping the total elongation of the supercell fixed. Again, this corresponds to a mode I cleavage process, but now elastic energy is released due to atomic relaxations.

III. UNIVERSAL BEHAVIOR AND SCALING LENGTHS

Rose et al.⁷ postulated and demonstrated that the binding energies E_b of metals have a universal form of the kind

$$E_b(d) = |E_b^e|g(a) \quad (6)$$

where d is the interatomic distance, or, in the case of interface energies the interplanar spacing. $|E_b^e|$ is the binding energy at equilibrium volume ($= -W_{\text{sep}}$) and a is the rescaled displacement

$$a = \frac{\Delta}{l} . \quad (7)$$

The characteristic length scale l depends on the curvature of the energy-volume curve at the minimum, i.e., on the elastic modulus as follows,

$$l = \sqrt{\frac{|E_b^e|}{E_b''(d_0)}} . \quad (8)$$

If rescaled in this manner, all energy-volume curves coincide, i.e. they have the same functional form $g(a)$. This phenomenon was observed for adhesion⁹ and cohesion¹⁰ of metals, as well as chemisorption on metal surfaces¹¹. More recently, Hayes et al. have shown that even the energy-displacement curves of non metallic systems (Al_2O_3 and Si) can be brought into coincidence with those of metals (Al)¹². This universal behavior of chemically different systems means that we can determine the cohesive behavior (i.e. theoretical strength and critical displacement) of any material from three parameters, E_b^e , d_0 , and $E_b''(d_0)$, once the functional form $g(a)$ is known. To describe hydrostatic volume expansion / compression of simple metals, Rose determined $g(a)$ to be

$$g(a) = -(1 + a + 0.05a^3)e^{-a} . \quad (9)$$

Hayes et al. used an asymptotic approximation, i.e. a simple quadratic function introduced by Nguyen et al.¹³ that scales with the system size to fit results of uniaxial computational tensile tests. Originally applied to the results of homogeneous strain, the approach was generalized by Hayes et al. to fit the results of tensile tests in the form of rgs + atomic relaxation, thus taking into account surface relaxations¹². The simple function and the scalability of the results make this approach attractive for the calculation of traction-separation laws used in continuum models. However, if the theoretical strength shall be calculated independently of the system size, a function displaying an inflection point is to be preferred. To fit the results of our tensile tests in the form of rigid grain shifts, we used

$$g(a) = -(1 + a)e^{-a} , \quad (10)$$

a function also used by Rose, to represent the results of displacing metal-metal interfaces of different metals.

IV. RESULTS

A. Grain boundary structures

After construction according to the macroscopic parameters the microscopic degrees of freedom of the grain

	d_0 [Å]	l_b [Å]	l_r [Å]
(111) bulk	-	0.561	1.652
(112) bulk	-	0.653	1.599
(113) bulk	-	0.655	1.695
(114) bulk	-	0.665	1.657
$\Sigma 3(111)[111]60^\circ$ twist GB	0.014	0.615	1.745
$\Sigma 3(1\bar{1}2)[110]109^\circ$ STGB	0.389	0.621	1.736
$\Sigma 11(1\bar{1}3)[110]129^\circ$ STGB	0.311	0.620	1.508
$\Sigma 9(1\bar{1}4)[110]141^\circ$ STGB	0.185	0.605	1.514

TABLE I: Excess volume at the different grain boundaries, represented by d_0 , and scaling lengths for brittle and relaxed cleavage, l_b and l_r , for bulk and grain boundary planes (explanation in the text).

boundaries were optimized by performing rigid grain shifts perpendicular as well as parallel to the interface, followed by relaxation of the atomic positions. All grain boundaries exhibit excess volume at the interface, calculated according to equation (2). These expansions d_0 are localized in the vicinity of the grain boundary, but not necessarily confined only to the first crystallographic plane at the interface. The expansions are summarized in table I. The smallest expansion is observed for the (111) twist grain boundary, which is the most dense cleavage plane after the (111) bulk plane. The stable translation state of the $\Sigma 11$ STGB parallel to the interface is the initial, mirror-symmetric one. In the case of the $\Sigma 3$ STGB a shift of 0.5 times the interplanar spacing along the tilt axis [110] breaks this mirror-symmetry and produces a structure about 150 mJ/m² lower in energy than the mirror-symmetric one. The $\Sigma 9$ STGB initially contained two atomic columns at unphysically small distance at the grain boundary. Relaxing the structure (rgs + atomic relaxations) led to major re-arrangements of the atomic positions at the interface. Removing instead one atomic column at the grain boundary and relaxing the structure (rgs + atomic relaxation) led to an interface energy which is lower by 0.067 Ha/atom (≈ 1.8 eV/atom). The resulting structure at the grain boundary is in excellent agreement with experimental observations¹⁴.

B. Interface energies and work of separation

The resulting interface energies, i.e. surface and grain boundary energies, and the work of separation for the systems investigated are shown in table II. The grain boundary energies follow the known trend for the energies of symmetric [110] tilt grain boundaries in fcc metals as function of the misorientation angle, with energy cusps representing the $\Sigma 3$ twist and the $\Sigma 11$ STGB^{3,4,15}. Results of previous DFT investigations were found for the $\Sigma 3$ twist¹⁶ and the $\Sigma 11$ STGB¹⁷ and agree well with our results. The work of separation for the grain boundaries

	γ [J/m ²]	W_{sep} [J/m ²]	σ_{th} [GPa]
(111) bulk	0.987	1.973	12.6
(112) bulk	1.109	2.218	12.8
(113) bulk	1.093	2.187	12.7
(114) bulk	1.145	2.290	13.2
$\Sigma 3(111)[111]60^\circ$ twist GB	0.048	1.924	11.5
$\Sigma 3(11\bar{2})[110]109^\circ$ STGB	0.393	1.818	6.8
$\Sigma 11(1\bar{1}3)[110]129^\circ$ STGB	0.171	2.007	12.0
$\Sigma 9(1\bar{1}4)[110]141^\circ$ STGB	0.486	1.779	12.1

TABLE II: Interface energy, work of separation, and theoretical strength of Al bulk and grain boundaries.

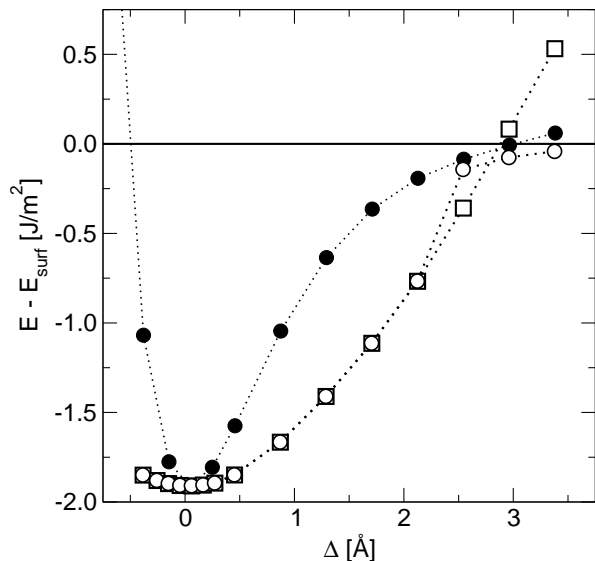


FIG. 1: Results of *ab initio* tensile tests along the [111] direction in bulk Al. Black circles represent the results of rgs, open circles that of rgs followed by relaxation of the atomic positions, and squares that of a homogeneous straining of the supercell.

does not follow the same trend, as it also depends on the corresponding surface energy. The lowest surface energy in Al is that of the close packed (111) plane. Thus, W_{sep} for the stable twin is lower than that of the $\Sigma 11$ STGB, corresponding to the second-most favorable [110] grain boundary orientation in fcc metals.

C. Energy-displacement curves

Starting from the optimized structures, tensile tests were performed as explained in section II. Figure 1 shows the results for bulk Al stretched and compressed along the [111] direction. Rigid grain shifts without any atomic relaxation produce a rather steep curve in a shape that can be fitted well by equation (10). The energy asymp-

totically approaches the unrelaxed (111) surface energy, which is slightly higher than the relaxed one taken as the reference energy level in fig. 1. After relaxing the atomic structure at each shift, the atomic positions and the corresponding energies coincide with the results obtained by stretching the supercell homogeneously. A deviation is observed above a relative displacement of the two bulk slabs of 2\AA . In the case of the rgs, the atoms relax to a configuration where the strain is localized at the defined cleavage plane, whereas in case of the homogeneous strain the crystallographic planes have the same distance. A continuation of the homogeneous tensile test would lead to N free standing crystallographic planes, if N is the number of layers in the supercell.

If the tensile test is performed with a supercell containing a grain boundary, the strain is expected to localize at this defect also in the case of a homogeneous elongation of the supercell. This is shown in figure 2 for the $\Sigma 11(113)[110]129^\circ$ symmetrical tilt grain boundary. Again, the black circles represent the results of the rigid grain shift calculations without atomic relaxations. The open circles mark the energies after atomic relaxation. The diamonds indicate the energies obtained after a successive scaling of the total length of the supercell, i.e. starting with the equilibrium structure the relaxed reduced coordinates of the atoms are taken as input coordinates of the next strain state. This ensures a continuous deformation path up to the point where the energy crosses the reference level, the energy of the relaxed (113) surface. At this point the energy drops and then starts to increase again. An analysis of the atomic structure at this discontinuity shows that the two grains have partially debonded and are only connected via chains of atoms containing the initial coincidence site. Due to this coincidence site a further elongation of the cell again leads to a free standing crystallographic plane, in the center between two (113) surfaces. Thus, while such a drag calculation is interesting to investigate failure modes and critical displacements, it is not suitable to calculate the work of separation or the tensile strength. We can conclude that for the latter a defined point of failure is needed in every loading scheme.

D. Scaling lengths for different geometries

As mentioned in section III, a universal behavior of materials under strain has been shown for bulk metals and ceramics, and for coherent metal-metal interfaces. In our investigation, we stick to one metal, Al, but probe different orientations of the tensile axis for bulk tensile tests, as well as different grain boundary geometries, where the tensile axis is perpendicular to the interface. As can be seen in figure 3 the results of rgs calculations scale perfectly. The parameters resulting from the fit are given in table II ($E_b = -W_{\text{sep}}$). For the case of rgs followed by atomic relaxations, the function given in equation (10) does not describe the results well. The fit could

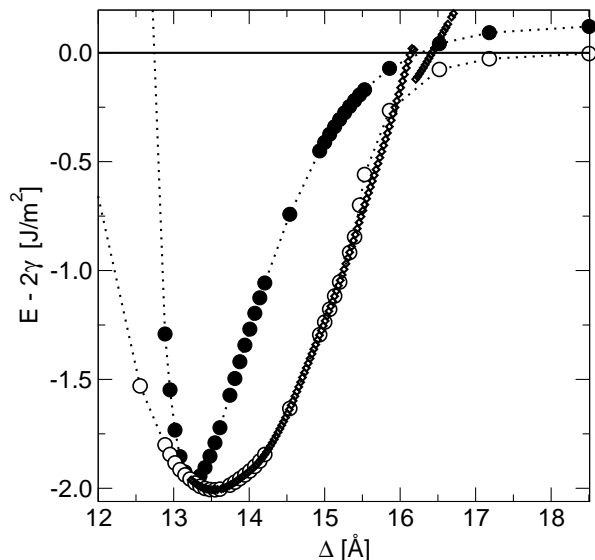


FIG. 2: Results of *ab initio* tensile tests at the Σ_{11} STGB. Black circles represent the results of rgs calculations without atomic relaxations, and open circles mark the energies after atomic relaxation. Diamonds are the energies obtained via a “drag” calculation (see text). The reference level is the energy of the relaxed (113) surface.

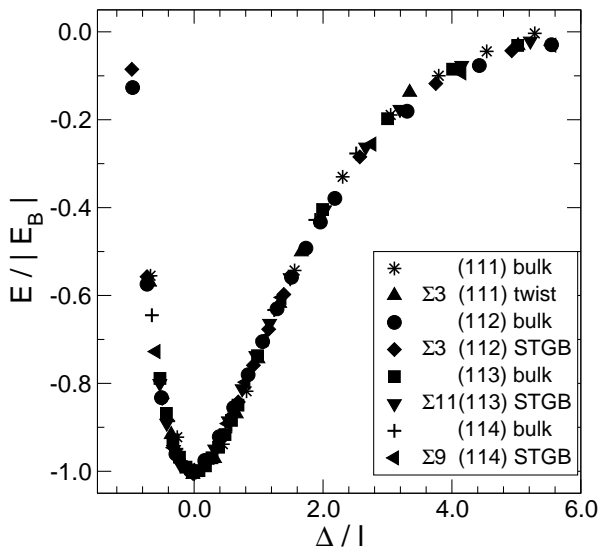


FIG. 3: Rgs energy displacement relationships re-scaled according to eqs. 6 to 8, using eq. 10. For details of the twist and STGB geometries see text.

be improved by using a polynomial including higher order terms (≥ 3). However, for the rescaling procedure the exact function $g(a)$ actually does not have to be known. Instead we determined the curvature at minimum energy by assuming a quadratic function close to the minimum, i.e. making a harmonic approximation. The results of rgs calculations followed by atomic relaxations were rescaled with the curvature thus obtained and with the binding energy. The rescaled curves are shown in figure

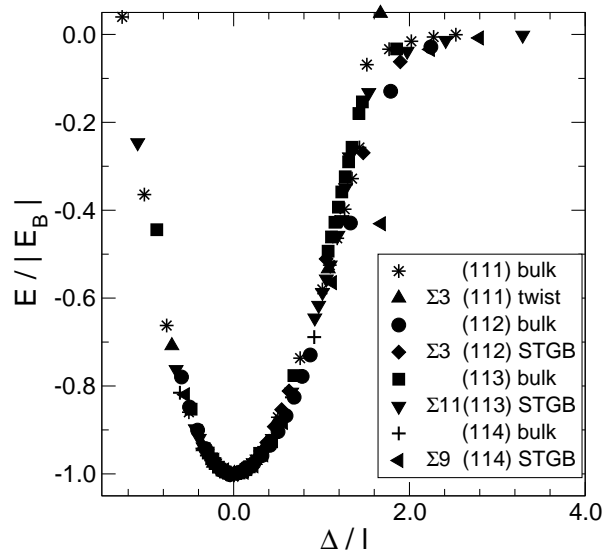


FIG. 4: Energy displacement relationships with relaxed atomic positions, re-scaled according to eqs. 6 to 8, using the harmonic approximation for $g(a)$. For details of the twist and STGB geometries see text.

4. Apart from a few outliers the agreement is satisfactory. Deviations occur mainly at displacements where the structure becomes unstable and where we can think of a crack forming. Thus, whether investigating relaxed or unrelaxed cleavage of different geometries, all we have to know about a system to describe its elastic response upon tensile load are the binding energy in the specified cleavage plane and the elastic constant (resp. $E''(\Delta)$) for the tensile direction. Especially for the grain boundaries we can conclude that once we have determined a fitting function $g(a)$ we can use it for the complete parameter space spanned by the degrees of freedom of the interfaces.

The scaling lengths calculated to make the different energy-displacement curves coincide are given in table I. For ideally brittle cleavage (rgs without atomic relaxation), the results for bulk Al agree very well with the empirical results of Rose et al.⁷, 0.66\AA . This value was obtained by using the experimental results of Simmons and Wang¹⁸ for the elastic constant of Al along the [111] direction and the surface energy of Tyson and Miller¹⁹. The latter represents an average over different crystallographic planes, thus we expect our value to be more exact. *Ab initio* calculations for bulk Al have been carried out by Lazar et al.²⁰. For tensile tests along the [111] direction they obtain $l_b = 0.54\text{\AA}$ and $l_r = 2.4\text{\AA}$. While there is excellent agreement between the scaling lengths for brittle cleavage, our result for the relaxed cleavage, also shown in table I, is about 30% lower. This is due to the fact that, although the energy-displacement curve is fitted to a quadratic function in both cases, the definition of l_r is different. Lazar and Podlucky²⁰ define l_r as the critical opening, at which the elastic energy $E(\Delta)$ equals the work of separation, comparable to the discontinuity in our drag results, see figure 1. This means their

quadratic fit is performed in the spirit of the asymptotic approximation of Nguyen and Ortiz¹³, however it is independent of the system size. In our case, where the quadratic fit is strictly confined to the region around the energy minimum, l_r has no such meaning, but is simply a measure for the stiffness of the cleavage plane, as in the work of Rose et al.

E. Tensile strength

From the derivatives of the energy-displacement curves, the theoretical tensile strength of the bulk phase along a given tensile axis and of grain boundaries along an axis perpendicular to the grain boundary plane, can be calculated according to equation (5). For direct comparison of bulk and grain boundary properties, we restrict ourselves to the results of rgs calculations without relaxation of the atomic positions. Thus, the strain is fully localized between the cleavage planes in both cases. A relaxation would lead to different strain distributions in the supercell, as discussed in detail in section II. The results are summarized in table II. The theoretical strength of a grain boundary is generally lower than that of bulk lattice planes in the corresponding orientation. Furthermore, in the bulk, the trend in theoretical strength follows the one in the work of separation: the higher W_{sep} , the higher σ_{th} . For the grain boundaries, however, although the same overall trend is still visible, the relationship is not so straight forward.

V. SUMMARY AND CONCLUSIONS

We have performed *ab initio* tensile tests of bulk Al along different tensile axes, as well as perpendicular to different grain boundaries. It has been discussed that in order to simulate a physically meaningful de-cohesion process, a plane of cleavage has to be defined in all systems, also those containing defects as grain boundaries. This was done by performing the tensile tests by means of rigid grain shifts, followed or not by relaxation of the atomic positions at each shift. The mechanical properties of the investigated systems are summarized again in figure 5. The grain boundary energies agree well with the empirical extension of the Read-Shockley picture, showing cusps at the $\Sigma 3$ (111) and the $\Sigma 11$ (113) orientations. The most stable defect judging from the interface energy is the (111) twist grain boundary. However, this is not the grain boundary with the highest strength, demonstrating that for defect structures as grain boundaries,

there is no simple relation between energy and strength, and σ_{th} has to be calculated explicitly.

Fortunately, it is not necessary to calculate full energy-displacement curves for the complete parameter space of grain boundaries, because, as we were able to show, these exhibit a universal behavior. Thus, after having determined the analytical function $g(a)$ once, we only need to

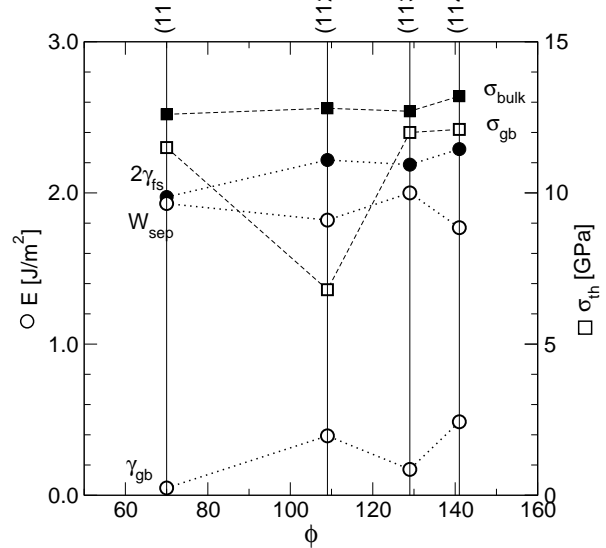


FIG. 5: Mechanical properties of the different grain boundaries and bulk supercells as function of the misorientation from (110). Energies are represented by circles, and stresses by squares. Grain boundary properties are displayed in white, and bulk and surface properties in black. For more explanations see text.

determine the minimum energy structure, corresponding surface energies, and the curvature at the minimum. By this simplification a use of *ab initio* tensile strengths in continuum models of polycrystals is getting within reach.

Acknowledgments

The authors thank Christian Elsässer for valuable comments on the UBER. Furthermore the authors acknowledge financial support through ThyssenKrupp AG, Bayer MaterialScience AG, Salzgitter Mannesmann Forschung GmbH, Robert Bosch GmbH, Benteler Stahl/Rohr GmbH, Bayer Technology Services GmbH and the state of North-Rhine Westphalia as well as the European Commission in the framework of the European Regional Development Fund (ERDF).

* Electronic address: rebecca.janisch@rub.de

¹ Y. Wei and L. Anand, *J. Mech. Phys. Solids* **52**, 2587 (2004).

² R. H. Kraft, J. F. Molinari, K. T. Ramesh, and D. H. Warner, *J. Mech. Phys. Solids* **56**, 2618 (2008).

³ A. P. Sutton and R. W. Balluffi, *Interfaces in Crys-*

- talline Materials*, new ed. (Oxford University Press, Oxford, 2006).
- ⁴ D. Wolf, *Scripta Metall.* **23**, 1713 (1989).
 - ⁵ A. P. Sutton and R. W. Balluffi, *Acta Metall.* **35**, 2177 (1987).
 - ⁶ D. L. Olmsted, S. M. Foiles, and E. A. Holm, *Acta Mater.* **57**, 3694 (2009).
 - ⁷ J. H. Rose, J. R. Smith, and J. Ferrante, *Phys. Rev. B* **28**, 1835 (1983).
 - ⁸ X. Gonze, B. Amadon, P.-M. Anglade, J.-M. Beuken, F. Bottin, P. Boulanger, F. Bruneval, D. Caliste, R. Caracas, M. Côté, T. Deutsch, L. Genovese, P. Ghosez, M. Giantomassi, S. Goedecker, D. Hamann, P. Hermet, G. Jollet, S. Leroux, M. Mancini, S. Mazevet, M. Oliveira, G. Onida, Y. Pouillon, T. Rangel, G.-M. Rignanese, D. Sangalli, R. Shaltaf, M. Torrent, M. Verstraete, G. Zerah, and J. Zwanziger, *Comput. Phys. Commun.* **180**, 2582 (2009).
 - ⁹ J. Ferrante and J. R. Smith, *Phys. Rev. B* **19**, 3911 (1979).
 - ¹⁰ J. H. Rose, J. R. Smith, F. Guinea, and J. Ferrante, *Phys. Rev. B* **29**, 2963 (1984).
 - ¹¹ J. R. Smith, J. Ferrante, and J. H. Rose, *Phys. Rev. B* **25**, 1419 (1982).
 - ¹² R. L. Hayes, M. Ortiz, and E. A. Carter, *Phys. Rev. B* **69**, 172104 (2004).
 - ¹³ O. Nguyen and M. Ortiz, *J. Mech. Phys. Solids* **50**, 1727 (2002).
 - ¹⁴ D. A. Muller and M. J. Mills, *Mat. Sci. Eng. A* **260**, 12 (1999).
 - ¹⁵ D. Saylor, B. E. Dasher, A. Rollet, and G. Rohrer, *Acta Mater.* **52**, 3649 (2004).
 - ¹⁶ L. Lymperakis, M. Friák, and J. Neugebauer, *Eur. Phys. J. Special Topics* **177**, 41 (2009).
 - ¹⁷ A. F. Wright and S. R. Atlas, *Phys. Rev. B* **50**, 15248 (1994).
 - ¹⁸ G. Simmons and H. Wang, *Single Crystal Elastic Constants and Calculated Aggregate Properties. A Handbook*, 2nd ed. (MIT, Cambridge, 1971).
 - ¹⁹ W. R. Tyson and W. A. Miller, *Surf. Sci.* **62**, 267 (1977).
 - ²⁰ P. Lazar and R. Podloucky, *Phys. Rev. B* **78**, 104114 (2008).